# Coalescence of Spreading Droplets on a Wettable Substrate

W. D. Ristenpart,[1] P. M. McCalla,[2] R. V. Roy,[3] and H. A. Stone[1,*]

[1]*Division of Engineering and Applied Sciences, Harvard University, Cambridge, Massachusetts 02138, USA*
[2]*Department of Physics, Morgan State University, Baltimore, Maryland 21251, USA*
[3]*Department of Mechanical Engineering, University of Delaware, Newark, Delaware 19716, USA*

(Received 24 February 2006; published 7 August 2006)

We investigate experimentally and theoretically the coalescence dynamics of two spreading droplets on a highly wettable substrate. Upon contact, surface tension drives a rapid motion perpendicular to the line of centers that joins the drops and lowers the total surface area. We find that the width of the growing meniscus bridge between the two droplets exhibits power-law behavior, growing at early times as $t^{1/2}$. Moreover, the growth rate is highly sensitive to both the radii and heights of the droplets at contact, scaling as $h_o^{3/2}/R_o$. This size dependence differs significantly from the behavior of freely suspended droplets, in which the coalescence growth rate depends only weakly on the droplet size. We demonstrate that the scaling behavior is consistent with a model in which the growth of the meniscus bridge is governed by the viscously hindered flux from the droplets.

DOI: 10.1103/PhysRevLett.97.064501 PACS numbers: 47.55.D−, 47.15.G−, 68.15.+e

Research on drop coalescence has focused on the case of two spherical drops or bubbles floating in fluid [1–3]. Coalescence also occurs, however, between drops located on solid substrates. The coalescence process on substrates consists of two stages: an initial rapid growth of a meniscus bridge between the droplets, and a slow rearrangement of the combined droplet shape from elliptical to more circular at longer times. Previous work on the coalescence of sessile drops has focused on the latter stage [4–6], but the dynamics of the first stage are crucial to applications where drops impinge, condense, or spread on substrates. For example, in spray painting and spray coating the material properties of the resulting solid coating depend sensitively on the extent of coalescence before fluid motion is hindered by other physical processes (e.g., solidification due to cooling or solvent evaporation) [7,8]. Similarly, liquid and chemical imbibition on plant foliage is directly affected by drop coalescence, since drops drain off by gravity upon reaching a critical weight [9,10]. At smaller length scales, a primary objective of microfluidic devices is to study chemical or biological kinetics in small volumes by rapidly mixing two droplets with different reactants [11,12]; several techniques have been developed to maneuver sessile droplets toward one another so that they may coalesce [13–16]. Despite the broad range of phenomena affected by drop coalescence on substrates, the influence of geometric and material parameters on the coalescence behavior on substrates has remained obscure.

In this Letter, we investigate the early-time coalescence dynamics of thin viscous droplets spreading due to surface tension on a flat, wettable substrate. We show experimentally and numerically that in the limit where the initial heights of the droplets (just prior to coalescence) are small compared to their radii ($h_o \ll R_o$) the time-dependent width $d_m(t)$ of the meniscus bridge between the two merging droplets (each with viscosity $\mu$ and surface tension $\gamma$) is governed by a simple scaling law, $d_m \sim (\gamma h_o^3 t/\mu R_o^2)^{1/2}$. This scaling is consistent with an elementary mass conservation model in the context of the lubrication approximation, wherein the meniscus growth is limited by the viscously hindered flux from the droplets. Surprisingly, details about the curvature of the meniscus bridge are not necessary to predict the meniscus growth, despite the putative role of the meniscus curvature in driving the coalescence process. This suggests that thin-film coalescence might be similarly calculable in other more complex geometries (e.g., multiple droplets or droplets on cylindrical fibers). Although many systems of interest involve equilibrium contact angles larger than those studied here, the results for the limiting case of infinitesimal angles should establish a lower bound for the coalescence rate of droplets with larger contact angles.

Our experimental setup (Fig. 1) consisted of adjacent silicone oil droplets placed on transparent polystyrene petri dishes (Falcon brand No. 353003). Prior to each experiment, a fresh petri dish was rigorously washed with deter-

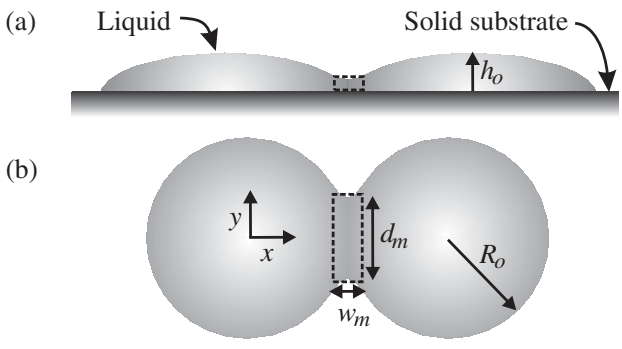


FIG. 1. Sketch of two thin droplets coalescing on a flat substrate. (a) Elevation view. (b) Plan view. Dashed lines indicate the control volume around the meniscus bridge.

 

gent, ethanol, and deionized water and then dried with filtered nitrogen gas. Three different silicone oils (Sigma Aldrich polydimethylsiloxane 200® fluid, $\gamma \approx 20$ mN/m) with viscosities of 100, 350, and 1000 cS were used as provided. The apparent equilibrium contact angle of each silicone oil on the polystyrene substrate was close to zero; given enough time, droplets spread over the entire petri dish. The droplet heights in our experiments never exceeded 0.5 mm, justifying neglect of gravitational effects in the analysis below.

To begin an experiment, a multitip hand pipetter with two disposable pipette tips was used to simultaneously deliver two droplets of oil to the substrate about 10 mm apart. The delivered volume of each droplet was approximately 20 $\mu$L; consistent reproducibility in droplet volume was difficult due to the tendency of the oil to wet the pipette tips. The coalescence dynamics were then observed with an optical microscope (Leica DM-IRB) using a phase-contrast objective and recorded with a CCD camera. The apparent contact lines were extracted from the recorded images using standard image analysis techniques.

A typical coalescence experiment is presented in Fig. 2. Prior to contact, the droplets spread radially [Fig. 2(a) and 2(b)]. Only a fraction of each droplet was within the microscope field of view, but enough was visible to calculate the growing radius of each droplet. Experiments where either the radii or the precoalescence spreading velocities of the two droplets differed by more than 10% from one another were excluded from analysis. Comparison of best-fit circles to the droplet contact line consistently yielded agreement to within $\pm 1$ pixel, indicating that the flow was radial and fully developed prior to coalescence.

Upon contact [Fig. 2(b)], the meniscus bridge grew out rapidly in the direction normal to the droplet line of centers [Fig. 2(c)–2(e)]. As time progressed, the velocity of the growing meniscus decreased. At very long times ($>30-60$ min), the combined elliptical droplet arranged into a more circular shape. Here we focus on the early-time dynamics, as depicted in Fig. 2.

The meniscus bridge width $d_m(t)$ is plotted as a function of time for three different viscosities (19 total experiments) in Fig. 3(a). The data indicate two important aspects of the coalescence behavior. First, the coalescence process is viscously dominated. Although there is overlap in the data, on average the 100 cS oil coalesced more rapidly than the 350 cS oil, which coalesced more rapidly than the 1000 cS oil. Second, there is a significant degree of variability between experimental trials with the same liquid: the apparent velocities differ by as much as a factor of 5 for ostensibly identical conditions.

To make sense of this scatter in the data, it is instructive to examine the governing equations for the evolution of thin films. In the lubrication limit, the height $h$ of a thin liquid film is governed by the fourth-order partial differential equation [17]

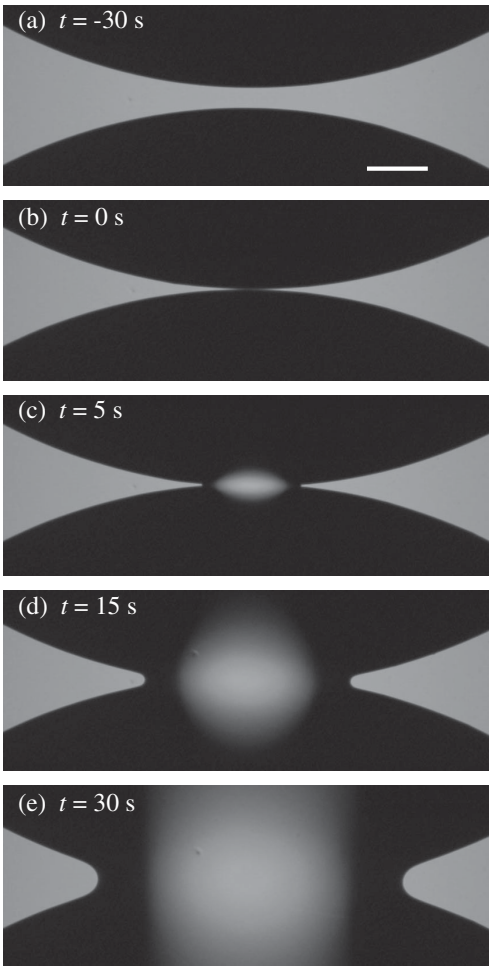


FIG. 2. Optical microscopy images of two silicone oil droplets ($\eta = 1000$ cS) spreading and coalescing on a flat polystyrene substrate. Dark regions are oil, light regions are background. Note that the droplet centers are outside the field of view. In later images, the light "halo" in the center of the oil is an artifact due to the decreased curvature with respect to the incident light. Scale bar in (a) is 500 $\mu$m.

$$\frac{\partial h}{\partial t} = -\frac{\gamma}{3\mu}\nabla \cdot (h^3 \nabla \nabla^2 h), \tag{1}$$

where gravitational forces are neglected. Choosing characteristic length scales $h \sim h_o$ and $\nabla \sim 1/R_o$, where $h_o$ and $R_o$ are, respectively, the maximum height and radius of the drops defined at the time of contact ($t_o$), we identify the dimensionless time

$$\tau \equiv \frac{\gamma h_0^3}{\mu R_0^4}(t - t_o). \tag{2}$$

This expression suggests that the geometry of the droplets has a pronounced influence on the coalescence dynamics, so slight variations in the droplet volume may account for the scatter [Fig. 3(a)].

Rescaling the data using $\tau$ requires a measurement of the droplet heights, but with the camera oriented perpendicu-

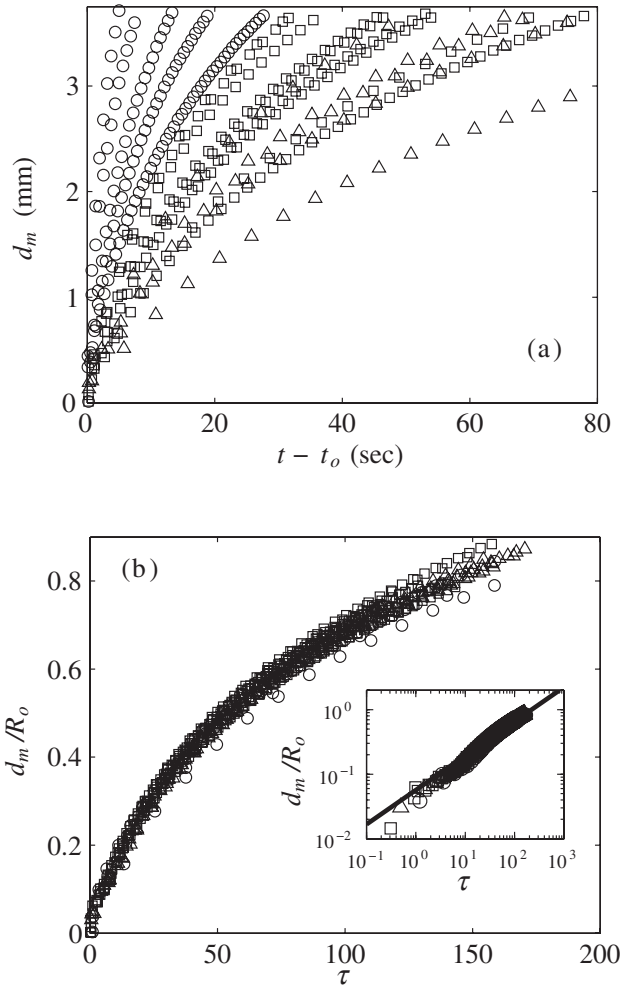


FIG. 3. (a) Width of the meniscus bridge versus time for three different viscosities. Symbols: ○, 100; □, 350; △, 1000 cS. Data represent 19 separate experiments; $t_o$ is the time of initial contact. (b) Width of the meniscus bridge in scaled coordinates, using all of the data presented in (a). Inset: logarithmic scale, fit slope = 0.53.

larly to the substrate the height could not be measured directly from the experimental images. However, after delivery to the substrate the total volume of each droplet is constant, so the height is related to the spreading velocity via Tanner's law [18], $\dot{R} \approx (\gamma/\mu)(h/R)^3$, which upon rearrangement yields $h \approx R(\mu\dot{R}/\gamma)^{1/3}$. Although not quantitatively accurate, this expression does incorporate the effect of variable height by means of the experimentally observable spreading velocity. Measurements of the precontact spreading velocities reveal a strong correlation with the post-contact coalescence velocities (data not shown), suggesting that the initial droplet height affects the coalescence speed.

To test the proposed time scaling, the meniscus widths were scaled by $R_o$ and time rescaled as $\tau$, using Tanner's law to estimate the height as $h_o \sim R_o(\mu\dot{R}_o/\gamma)^{1/3}$. Rescaling the data in this manner collapses the data onto a master curve [Fig. 3(b)]. Furthermore, when the results are plotted on a log-log scale, the best-fit slope for $d_m \propto \tau^\alpha$ yields $\alpha = 0.53$ [Fig. 3(b), inset].

To further explore this power-law response, we investigated Eq. (1) numerically using a finite-difference method [19]. The domain consisted of two spreading droplets, of initial radius $R_*$ and initial height $h_*$, with a symmetry plane down the line of centers. Slip on the solid substrate was modeled by means of a thin precursor film of thickness $h_\infty \ll h_*$ through the remainder of the domain; in this manner complexities associated with the moving contact line are avoided. Preliminary calculations confirmed that Tanner's law is recovered for a single spreading droplet in the limit as $\delta = h_*/h_\infty \to 0$. The numerical results for coalescing drops show that the early meniscus growth is indeed characterized by a power law $\tau^{1/2}$, consistent with the experimental results (Fig. 4).

Although the experimental and numerical results suggest that the growing meniscus bridge obeys a power-law scaling with exponent 1/2, the physical explanation for this result is not obvious *a priori* from the governing equation. The scaling behavior is explicable, however, in terms of a mass balance on the growing meniscus bridge. For the incompressible flows under consideration here, the change of volume of the meniscus bridge is balanced by the fluid flux into it, viz.

$$\frac{dV_m}{dt} \approx \langle u \rangle A_m. \tag{3}$$

Here the control volume is approximated by a rectangular box of length $d_m$, width $w_m$, and average height $h_m$ [cf. Fig. 1]. An exact definition of $h_m$ is unimportant since it does not affect the final result. Fluid only enters the

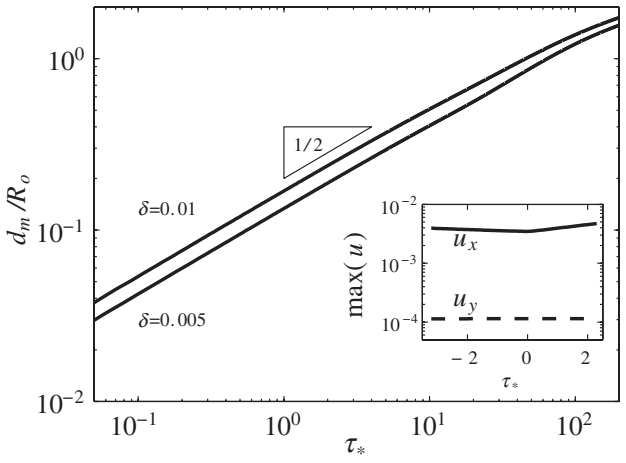


FIG. 4. Numerical calculations of the meniscus width vs dimensionless time, $\tau_* = \gamma h_*^3(t - t_o)/\mu R_*^3$, for two different precursor film thicknesses. Inset: numerical calculations of the depth-averaged velocities versus time. Solid line: the maximum $x$ velocity calculated on the $x$ axis (the line joining the drop centers). Dashed line: the maximum $y$ velocity on the axis at the point of contact ($x = R_o$).

control volume through the sides facing the two droplets, each with area $A_m \sim d_m h_m$. Likewise, the volume $V_m$ is approximately $V_m \sim d_m w_m h_m \sim d_m^3 h_m / R_o$, where the latter equivalence follows from a series expansion for $w_m$, valid for $d_m \gg w_m$. Rearrangement of Eq. (3) and substitution of the dimensionless time scale [cf. Eq. (2)] yields the dimensionless expression $d_m^2 \sim \tau \langle u \rangle$, where the velocity is scaled on the Tanner's law velocity.

It is noteworthy that for time-independent average velocities, the mass balance already yields the scaling relation $d_m \sim \tau^{1/2}$. Our numerical calculations of the velocity field into and inside the meniscus bridge confirm that the average influx varies little over the time of interest (Fig. 4, inset). Prior to contact, the maximum $x$ velocity is a measure of the spreading velocity; after contact, it is a measure of the liquid flow into the meniscus. The key observation is that the influx velocity varies very slowly with time. Likewise, the maximum $y$ velocity is clearly negligible and unaffected by coalescence in the time interval shown, demonstrating that the initial phase of meniscus growth after contact is governed by the slow flux in the $x$ direction due to spreading.

It may seem surprising that a mass balance yields accurate scaling predictions for the meniscus growth, in spite of the neglect of details regarding the meniscus curvature. Indeed, for time invariant influx velocities, the mass conservation argument yields predictions equivalent to those obtained by calculating the intersection width of two adjacent circles whose radii increase linearly with time (as demonstrated by geometric arguments). It is important to note that there is no reason *a priori* to expect that the influx velocity is constant; for example, one might expect that the velocity is affected by complications associated with the overlap of the droplet precursor films or the initially infinite curvature of the meniscus. The key result of this work is that any such effects are negligible.

In summary, we find experimentally and numerically that the meniscus bridge between two spreading sessile drops grows as $d_m \sim (\gamma h_o^3 t / \mu R_o^2)^{1/2}$, which is consistent with a mass conservation model in the lubrication limit. Other coalescence phenomena might exhibit similar scaling behavior in situations where fluids spread toward one another. For example, spreading of thin drops driven by gravity rather than surface tension should exhibit similar scaling; a numerical study by Diez and Kondic suggests that the meniscus bridge indeed increases as $t^{1/2}$ in the case of gravitational spreading [20]. Likewise, drop coalescence in porous media or on highly curved substrates might be amenable to such analysis since the velocities of individually spreading droplets are well characterized.

In the context of droplets on flat substrates, it is instructive to compare the obtained scaling for thin films with that of freely suspended liquid spheres. As discussed by Eggers *et al.* [2], the radius of the meniscus bridge between two coalescing liquid spheres grows linearly with time, with a weak (logarithmic) dependence on the drop radii. According to the present results, thin droplets on substrates coalesce much more slowly with a strong (power-law) dependence on their geometry. Presumably the coalescence behavior of sessile droplets with very large contact angles (close to 180°) is more similar to that of freely suspended spheres than thin droplets. This suggests that the scaling law obtained here serves as a lower bound for estimating the coalescence rate of sessile droplets with larger contact angles.

This work was supported by the Harvard MRSEC (No. DMR-0213805), and support for P. M. M. was provided by the REU program. We thank A. Ajdari for suggesting analysis of the dynamics with intersecting circles and for a critical review of the manuscript.

*Electronic address: has@deas.harvard.edu

[1] J. Frenkel, J. Phys. (USSR) **9**, 385 (1945).
[2] J. Eggers, J. R. Lister, and H. A. Stone, J. Fluid Mech. **401**, 293 (1999).
[3] D. Aarts, H. N. W. Lekkerkerker, H. Guo, G. H. Wegdam, and D. Bonn, Phys. Rev. Lett. **95**, 164503 (2005).
[4] C. Andrieu, D. A. Beysens, V. S. Nikolayev, and Y. Pomeau, J. Fluid Mech. **453**, 427 (2002).
[5] S. J. Gokhale, S. DasGupta, J. L. Plawsky, and P. C. Wayner, Phys. Rev. E **70**, 051610 (2004).
[6] R. Narhe, D. Beysens, and V. S. Nikolayev, Langmuir **20**, 1213 (2004).
[7] J. Madejski, Int. J. Heat Mass Transf. **19**, 1009 (1976).
[8] T. H. Van Steenkiste, J. R. Smith, R. E. Teets, J. J. Moleski, D. W. Gorkiewicz, R. P. Tison, D. R. Marantz, K. A. Kowalsky, W. L. Riggs, and P. H. Zajchowski *et al.*, Surf. Coat. Technol. **111**, 62 (1999).
[9] H. B. Tukey, Ann. Rev. of Plant Physiology **21**, 305 (1970).
[10] M. Knoche, Crop Protection **13**, 163 (1994).
[11] H. Song, J. D. Tice, and R. F. Ismagilov, Angew. Chem., Int. Ed. **42**, 768 (2003).
[12] H. A. Stone, A. D. Stroock, and A. Ajdari, Annu. Rev. Fluid Mech. **36**, 381 (2004).
[13] D. F. Dos Santos and T. Ondarçuhu, Phys. Rev. Lett. **75**, 2972 (1995).
[14] K. Ichimura, S. K. Oh, and M. Nakagawa, Science **288**, 1624 (2000).
[15] S. K. Cho, H. J. Moon, and C. J. Kim, J. Microelectromech. Syst. **12**, 70 (2003).
[16] A. A. Darhuber, J. P. Valentino, J. M. Davis, S. M. Troian, and S. Wagner, Appl. Phys. Lett. **82**, 657 (2003).
[17] A. Oron, S. H. Davis, and S. G. Bankoff, Rev. Mod. Phys. **69**, 931 (1997).
[18] L. H. Tanner, J. Phys. D: Appl. Phys. **12**, 1473 (1979).
[19] L. W. Schwartz, R. V. Roy, R. R. Eley, and S. Petrash, J. Colloid Interface Sci. **234**, 363 (2001).
[20] J. A. Diez and L. Kondic, J. Comput. Phys. **183**, 274 (2002).